Cancer Management and Research

Dovepress
open access to scientific and medical research

Open Access Full Text Article

ORIGINAL RESEARCH

Comparison of Diagnostic Efficacy Between Contrast-Enhanced Ultrasound and DCE-MRI for Mass- and Non-Mass-Like Enhancement Types in Breast Lesions

This article was published in the following Dove Press journal:
Cancer Management and Research

Wei Liu[1,*]
Min Zong[2,*]
Hai-yan Gong[1,*]
Li-jun Ling[3]
Xin-hua Ye[1]
Shui Wang[3]
Cui-ying Li[1]

[1]Department of Ultrasound, The First Affiliated Hospital of Nanjing Medical University, Nanjing 210029, People's Republic of China; [2]Department of Radiology, The First Affiliated Hospital of Nanjing Medical University, Nanjing 210029, People's Republic of China; [3]Department of Breast Surgery, The First Affiliated Hospital of Nanjing Medical University, Nanjing 210029, People's Republic of China

*These authors contributed equally to this work

Correspondence: Cui-ying Li
Department of Ultrasound, The First Affiliated Hospital of Nanjing Medical University, No. 300, Guangzhou Road, Nanjing 210029, People's Republic of China
Tel +86-15062260771
Email lcy_njmu@163.com

Shui Wang
Department of Breast Surgery, The First Affiliated Hospital of Nanjing Medical University, No. 300, Guangzhou Road, Nanjing 210029, People's Republic of China
Tel +86-13701458115
Email wangshui_njmu@163.com

Background: Contrast-enhanced ultrasound (CEUS) can provide angiogenesis information about breast lesions; however, its diagnostic performance in comparison with that of dynamic contrast-enhanced magnetic resonance imaging (DCE-MRI) has not been systematically investigated. This study aimed to evaluate the diagnostic efficacy of CEUS and DCE-MRI in mass-like and non-mass-like enhancement types of breast lesions.

Material and Methods: A retrospective study was conducted on 252 patients with breast lesions who underwent CEUS and DCE-MRI before surgery between January 2016 and February 2020. Histopathological results were used as reference standards. All patients were classified into mass-like and non-mass-like enhancement lesion groups. The mass-like lesion group was further divided into three categories according to different sizes (group 1: <10 mm, group 2: 10–20 mm, and group 3: >20 mm). Sensitivity, specificity, positive predictive value, negative predictive value, and receiver operating characteristic curve were analyzed to assess the diagnostic performance of these two modalities.

Results: For mass-like breast lesions, DCE-MRI (Az=0.981) manifested better diagnostic performance than CEUS (Az=0.940) in medium-sized (10–20 mm) tumors (Z=2.018, P=0.043), but both had similar diagnostic performance in smaller (<10 mm) and larger (>20 mm) tumors (P=0.717, P=0.394). For non-mass-like enhancement lesions, CEUS and DCE-MRI showed no significant difference (Z=1.590, P=0.119) and revealed good diagnostic performance (Az=0.859, Az=0.947) in differentiating the two groups.

Conclusion: For mass-like breast lesions, DCE-MRI showed better diagnostic performance than CEUS in differentiating benign and malignant tumors of medium-sizes (10–20mm) but not of smaller (<10mm) and larger (>20 mm) sizes. For non-mass-like lesions, both modalities showed similar diagnostic performance.

Keywords: contrast-enhanced ultrasound, dynamic contrast-enhanced MRI, mass-like breast lesion, non-mass-like breast lesion, breast cancer

Introduction

Breast tumors commonly occur in women, and breast cancer has become the first threat to women's health[1,2] and the leading cause of cancer deaths in most countries. Therefore, the diagnosis and treatment of breast cancer have become a global problem. Detecting and diagnosing breast cancer in early stages (tumor size <20 mm) greatly contributes to the prognosis[3–7] and is an effective strategy to

reduce mortality rate, extend patient survival time, and improve the quality of life. Breast lesions are divided into mass-like and non-mass-like types. Preoperative imaging diagnosis of non-mass-like lesions is difficult due to their complex imaging appearance, which also affects the formulation of treatment plans.[8–10]

As the most sensitive breast lesion examination method to date, dynamic contrast-enhanced magnetic resonance imaging (DCE-MRI) can comprehensively and systematically evaluate breast lesions. However, patients with some conditions, such as those who have a heart pacemaker, a metallic foreign body (metal sliver) in their chest position, and severe claustrophobia, cannot undergo the MRI examination.[11] In addition, gadolinium-containing contrast agents can lead to discomfort or become life-threatening for patients with sensitive constitutions. Ultrasound (US) is a commonly used imaging modality to detect breast lesions, especially for Asian women with fibrous gland breasts, and has become the main auxiliary modality.[12–15] Compared with MR imaging, the US has benefits, such as ultrafast examination and less susceptibility to patient motion. However, conventional US is not ideal for small lesions with a diameter <10 mm or with atypical morphologic features. Overlapping occurs between the characteristics of benign and malignant lesions as projected on conventional US scans.[16,17] Moreover, breast conventional US has limitations, such as in patients with high body habitus and the possibility of false-positive results.

Contrast-enhanced ultrasound (CEUS) can provide angiogenesis information about breast lesions. Angiogenesis is the common characteristic pathological process of most solid tumors and is related to tumor growth, invasion, metastasis, and prognosis.[18–20] The contrast agent component used by CEUS is SF6, a large-volume microbubble that can be confined in the blood vessel, does not enter the interstitial space, and can be metabolized out of the body through the lungs, and thus has relatively high safety. This agent has been widely used in the diagnosis of liver, prostate, and breast diseases because it can display the dynamic characteristics of neovascularization in the tumor.[21] Du and Li et al.[22,23] compared the diagnostic performance of CEUS and DCE-MRI and reported good agreement between these modalities in differentiating benign and malignant breast lesions. Xiang et al revealed that CEUS plus MRI could upgrade the diagnostic reliability for breast masses and fibroadenomas.[24] To date, the diagnostic performances of CEUS and DCE-MRI in non-mass-like lesions and mass-like lesions of different sizes have not been not systematically investigated and compared.

This study aimed to analyze the image characteristics and diagnostic efficacy of conventional US, CEUS, and contrast-enhanced MRI for breast diseases, especially for breast masses of different sizes and non-mass-like enhancement of breast lesions in DCE-MRI.

Materials and Methods

Study Population

This study was approved by the ethics committee of the First Affiliated Hospital of Nanjing Medical University (Nanjing, China). Informed consent was waived since this was a retrospective study and the study protocol conformed to the ethical guidelines of the Declaration of Helsinki. All patient data accessed complied with relevant data protection and privacy regulations. From January 2016 to February 2020, 259 female patients with breast diseases who first underwent conventional US + CEUS and then DCE-MRI examination were performed. The conventional US and CEUS examinations were performed simultaneously, and the relevant image features and diagnoses were obtained at one time. Inclusion criteria were as follows: (1) patients with primary breast cancer confirmed after surgery resection; (2) patients with primary with lesion characteristics and lymph node status on US; (3) patients did not accept an ipsilateral or contralateral history of malignant lesion surgery, radiotherapy, chemotherapy, or existing distant metastasis prior to imaging examination; (4) final histopathological results were acquired by surgery or US-guided core-needle biopsy at our hospital; and (5) the interval between the two examination modalities was not more than 2 weeks. Exclusion criteria were as follows: (1) history of previous ipsilateral breast cancer with axillary surgery or radiotherapy; (2) interval between the DCE-MRI examination and subsequent operation exceeded 1 month; (3) patients underwent neoadjuvant chemotherapy prior to image examination; and (4) patients with multifocal lesions or bilateral disease. Finally, 252 patients aged 23–88 years (mean age 47.15 ± 11.06 years) were included in this study.

Conventional US and CEUS

An US scanner (Mylab Twice, ESAOTE S.p.A. Italy) was used with a LA523 (5–13 MHz) linear transducer for conventional US and a LA522 (4–9 MHz) linear transducer for CEUS. CEUS was performed in contrast mode with

the second-generation contrast agent SonoVue (Italy, sulfur hexafluoride SF6). Esaote MYLAB US system was employed with the contrast mode of MI 0.07. The patient was lying flat with her hands raised, her upper arms perpendicular to the midline of the body, and the breasts and axillary on both sides were fully exposed. The injection needle was placed prior to the imaging, and the assistant added 5 mL of physiological saline for injection to the SonoVue freeze-dried powder and shaken the mixture to obtain a milky white liquid. The location of the mass was determined by the conventional US, and the probe was stabilized at the largest section of the mass. The US-operating doctor switched the contrast mode while injecting 2.4 mL of contrast agent through the cubital vein group and then injected 5 mL of saline into the flushing tube to dynamically observe the filling of the contrast agent in the mass. Mass changes after the contrast were recorded, and the dynamic images were retained.

MRI Examinations

MRI was performed using a Siemens 3.0T MRI instrument (Germany, MAGNETOM Spectra) with a bilateral eight-channel phased array breast coil while the patient laid in the prone position. Contrast agent Gd-DOTA (Gd-DOTA; Dotarem®; Guerbet, Roissy CdG Cedex, France) was administered. The sequences were as follows: (1) An axial turbo spin-echo T2-weighted imaging sequence with repetition time/echo time (TR/TE), 5000/61 ms; field-of-view (FOV), 320 mm × 320 mm; matrix size, 576 × 403; slice thickness, 4 mm; (2) A DWI sequence, read-out-segmented echo-planar imaging, with b-values, 50 and 800 s mm^{-2}; TR/TE, 5400/86 ms; FOV, 360 mm × 180 mm; matrix size,192 × 82; and slice thickness, 4 mm. Five readout segments were acquired for readout-segmented echo-planar imaging. ADC maps were calculated automatically by using MRI software from the DWI; (3) the dynamic series, consisting of a three-dimensional transverse fast low-angle shot T1-weighted sequence with fat suppression; TR/TE, 4.23/1.57 ms; FOV, 340 mm × 340 mm; flip angle, 10; matrix size, 448 × 296; slice thickness, 0.9 mm; and pixel resolution, 1.1 mm × 0.8 mm × 0.9 mm. Gadopentetate dimeglumine (Magnevist; Bayer Healthcare, Berlin, Germany) was administered intravenously as a bolus (0.1 mmol kg^{-1} body weight) by a power injector at 3.0 mL s^{-1}, followed by a 20 mL of saline flush after the pre-contrast acquisition. Images were acquired in five post-contrast acquisitions with no gap centered at 20 s within a total of 5 min and 41 s; and (4) Sagittal T2-weighted imaging sequence with fat suppression, TR/TE, 3000/72 ms; FOV, 340 mm × 340 mm; matrix size, 269 × 384; and slice thickness, 4.0 mm.

Table 1 Histopathologic Results of All Breast Lesions

Pathological Results	Mass-Like Lesions (n)			Non-Mass-Like Lesions (n)	Total (n)
	Size <10mm	Size 10–20mm	Size>20mm		
Benign (n=148)					
Fibrocystic breast disease	10	18	4	8	40
Fibroadenoma	10	27	20	11	68
Papilloma	7	3	1	0	11
Inflammation	3	1	3	1	8
Sclerosing adenopathy	4	0	3	0	7
Phyllodes tumor	6	0	1	0	7
Cyst	2	0	0	0	2
Aggressive fibromatosis	3	2	0	0	5
Malignant (n=104)					
Invasive ductal carcinoma	4	10	21	12	47
Intraductal carcinoma	0	8	3	9	20
Mucinous carcinoma	1	5	3	4	13
Invasive lobular carcinoma	0	3	6	4	13
Mixed carcinoma	0	1	0	0	1
Solid papillary carcinoma	1	2	0	0	3
Adenocarcinoma	0	1	0	0	1
Lymphoma	0	1	0	0	1
Carcinoma in situ	0	1	1	3	5

Image Analysis

CEUS images were collected and interpreted by two experienced US physicians, and DCE-MRI images were retrospectively interpreted by two experienced breast radiologists. All readers were blinded to surgical, histopathological, and other imaging findings prior to the evaluation. Each reader independently performed the assessment of morphological features and internal enhancement pattern. When disagreement occurred, then the readers jointly reviewed the images, discussed, and obtained a consensus. Clock method was used to record the position of breast lesions to ensure that the data of CEUS and DCE-MRI were of the same lesion. The lesions that showed non-mass-like enhancement on the MRI were classified into the non-mass group, and their scope and enhancement status were recorded, including the size or scope of the lesion, shape, margin, orientation, and enhancement status. The corresponding US+CEUS image features were also recorded, including the size or scope of the lesion, shape, margin, orientation, posterior echoes, and enhancement status. The mass-like lesions with various sizes were further classified into three groups of <10 mm, 10–20 mm, and >20 mm to study the diagnostic efficacy of CEUS and DCE-MRI for masses of different sizes. The pathological size was used as the standard for grouping. The upgrade or downgrade of CEUS diagnosis is based on conventional US. If the lesion shows hyperenhancement or heterogeneous on CEUS, it is upgraded; otherwise, it is downgraded. According to the American College of Radiology (ACR) Breast Imaging Reporting And Data System (BI-RADS) lexicon developed by the American College of Radiology to standardize mammographic reporting, the lesions were grouped into categories 3, 4A, 4B, 4C, and 5 with <2%, >2%–10%, >10%–50%, >50% but <95, and >95% likelihoods of malignancy, respectively. BI-RADS category 3 was labelled as 0.02, BI-RADS category 4A/4B/4C was labelled as 0.1, 0.5, and 0.95, and BI-RADS category 5 was labelled as 1 to ensure that the benign and malignant tendencies of different BI-RADS classifications were expressed. The ROC curve was drawn based on these values, and the diagnostic efficacy was calculated.

Statistical Analysis

SPSS19.0 data processor was applied. Normally distributed data were analyzed with *t*-test. Differences in CEUS and DCE-MRI imaging features and enhancement patterns between benign and malignant breast masses were evaluated by using Chi-square test (χ^2 test). Bonferroni correction was used for adjustment after multiple comparisons. Receiver operating characteristic (ROC) curve analysis was performed to compare the diagnostic performance of different modalities. The sensitivity, specificity, and overall accuracy of different modalities in the differential diagnosis of breast lesions were computed and compared using McNemar test. Confidence intervals (CI) for the area

Table 2 Comparison of CEUS and DCE-MRI Features Among Benign and Malignant Non-Mass-Like Enhanced Breast Lesions

Variables	Benign n (%)	Malignant n (%)	*P*
CEUS			<0.001
Shape			
Regular	10 (52.6)	9 (47.4)	
Irregular	8 (25.8)	23 (74.2)	
Margin			<0.001
Distinct	13 (72.2)	5 (27.8)	
Indistinct	5 (15.6)	27 (84.4)	
Orientation			<0.001
Parallel (height to width ratio <1)	15 (44.1)	19 (55.9)	
Not parallel (height to width ratio ≥1)	3 (11.5)	23 (88.5)	
Posterior echoes			0.007
None	11 (47.8)	12 (52.2)	
Shadowing (decreased posterior echoes)	7 (25.9)	20 (74.1)	
Enhance pattern			<0.001
Homogeneous	9 (25.7)	26 (74.3)	
Heterogeneous	9 (50.0)	9 (50.0)	
Enhancement degree			0.027
Hyperenhancement	11 (34.4)	21 (65.6)	
Hypoenhancement	7 (38.9)	11 (61.1)	
Radial or penetrating vessels			<0.001
Present	2 (8.0)	23 (92.0)	
Absent	16 (64.0)	9 (36.0)	
Expanded scope			<0.001
Yes	1 (4.3)	22 (95.7)	
No	17 (63.0)	10 (37.0)	
DCE-MRI			0.001
Enhance pattern			
Homogeneous	15 (53.6)	13 (46.4)	
Heterogeneous	3 (12.5)	21 (87.5)	
TIC curve			<0.001
Increasing type	11 (73.3)	4 (26.7)	
Plateau type	5 (41.7)	7 (58.3)	
Wash-out type	2 (8.0)	23 (92.0)	
ADC value ($10^{-3}mm^2/s$)	1.3±0.24	0.9±0.17	0.001

under the ROC curve (*Az*) values were estimated based on a 95% confidence level. For each analysis, a $P<0.05$ was considered to indicate a significant difference.

Results

Pathological results

All of 252 patients aged 23–88 years were included in this study. The pathological diagnoses were benign in 148 patients (mean age 43 years, range 34–52 years) and malignant in 104 patients (mean age 50 years, range 34–52 years). The patients were classified into non-mass -like and mass-like breast lesion groups. Patients with mass-like breast lesions were further divided into three groups according to size: <10, 10–20, and >20 mm. Table 1 presents the detailed pathological information of the benign and malignant tumors of different groups.

Image Features of Non-Mass-Like Enhanced Breast Lesions

Among the 52 non-mass-like enhancements of breast lesions, 2 had no manifestation on CEUS. Among the remaining 50 breast lesions, 37 out of fifty manifested as a mass with a sense of space, and 13 out of fifty cases manifested as irregular flaky hypoechoic. The detailed image features are presented in Table 2. Statistical differences in shape, margin, orientation, and posterior echoes were observed between benign and malignant lesions ($P<0.05$ for all). The non-mass-like enhancement of breast lesions showed special CEUS imaging characteristics, namely, the presence of radial or penetrating vessels and the enlarged lesion area compared with those on conventional US. These two characteristics frequently appeared in malignant breast lesions ($P<0.001$ for both). The enhancement pattern and degree of CEUS and DCE-MRI also had a statistical difference between the two groups. The difference between ADC values of DCE-MRI in benign and malignant lesions was statistically significant ($P < 0.001$). The mean ADC values of malignant lesions were $(0.90\pm 0.17) * 10^{-3}mm^2/s$ and $(1.3 \pm 0.24) * 10^{-3}mm^2/s$ in benign lesions. The representative non-mass-like case is shown in Figure 1A–D.

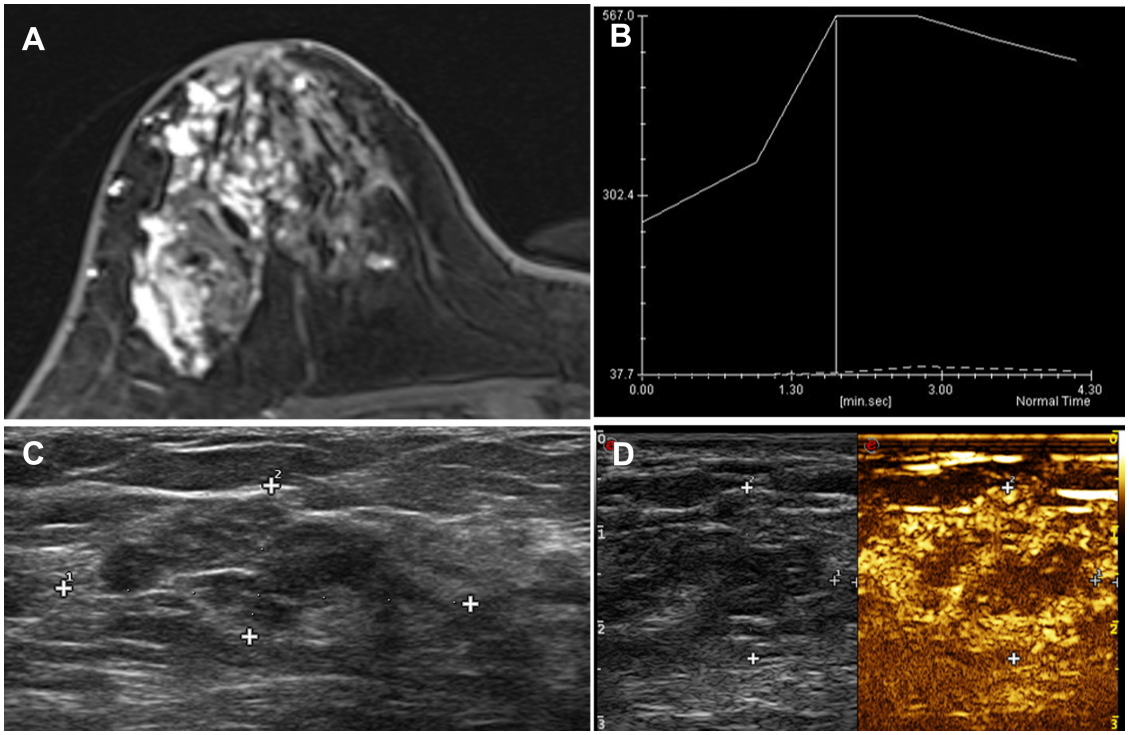

Figure 1 A 44-year-old female patient had progressive enlargement of her breast mass in the right upper outer quadrant for more than 1 year. (**A**) DCE-MRI showed a non-mass-like enhancement of about 86*32*43mm, and the boundary between the lesion and the surrounding structure is unclear. (**B**) The TIC curve was plateau type. (**C**) CEUS indicated that the heterogeneity of the right breast at 9 o'clock was a slightly hypoechoic nodule, (**D**) showing uneven hyperenhancement. The surrounding blood vessels were more disordered. An unenhanced area was found in the center, and the lesion area enlarged compared with conventional US. The pathology result is ductal carcinoma in situ (DCIS).

Table 3 Comparison of CEUS and DCE-MRI Features Among Benign and Malignant in Mass-Like Breast Lesions

Variables	Benign n (%)	Malignant n (%)	*P*
CEUS			<0.001
Shape			
Regular	76 (59.4)	5 (6.9)	
Irregular	52 (40.6)	67 (93.1)	
Margin			<0.001
Distinct	98 (76.6)	7 (9.7)	
Indistinct	30 (23.4)	65 (90.3)	
Orientation			0.004
Parallel (height to width ratio <1)	112 (87.5)	36 (50.0)	
Not parallel (height to width ratio ≥1)	16 (12.5)	36 (50.0)	
Posterior echoes			<0.001
None	91 (71.1)	48 (66.7)	
Decreased posterior echoes	0 (0.0)	18 (25.0)	
Increased posterior echoes	37 (28.9)	6 (8.3)	
Enhancement			
Enhancement pattern			0.003
Homogeneous	99 (77.3)	31 (43.1)	
Heterogeneous	29 (22.7)	41 (56.9)	
Enhancement degree			<0.001
Hyperenhancement	69 (53.9)	61 (84.7)	
Isoenhancement	21 (16.4)	4 (5.6)	
Hypoenhancement	38 (29.7)	72 (9.7)	
DCE-MRI			
Enhance pattern			0.005
Homogeneous	87 (68.0)	33 (45.8)	
Heterogeneous	41 (32.0)	39 (54.2)	
TIC curve			<0.001
Persistent	87 (68.0)	9 (12.5)	
Plateau	26 (20.3)	38 (52.8)	
Washout	15 (11.7)	25 (34.7)	
ADC value ($10^{-3}mm^2/s$)	1.4 ± 0.16	0.9 ± 0.24	0.002

Image Features of Mass-Like Breast Lesions

The enhancement characteristics of benign and malignant mass-like breast lesions are presented in Table 3. Statistical differences in shape, margin, orientation, and posterior echoes were observed between benign and malignant lesions (P <0.05 for all). The enhancement pattern and enhancement degree of the lesions in CEUS and DCE-MRI were significantly different between benign and malignant lesions (P < 0.05 for all). The difference between ADC values in benign and malignant lesions was statistically significant (P = 0.002). The mean ADC values were (0.93 ± 0.24) * $10^{-3}mm^2/s$ in the malignant group and (1.46 ± 0.16) * $10^{-3}mm^2/s$ in the benign group. The TIC curve of malignant lesions was mainly plateau type (or type 2 kinetics) and wash-out type (or type 3 kinetics) (39.3%, 29.7%), whereas that of benign lesions was mainly gradual and plateau type (53.6%, 25.0%). The difference was statistically significant (P<0.001). The representative mass-like cases with diameters >10 and <20 mm are shown in Figures 2A–D and 3A–D.

Comparison of Diagnostic Performance Between CEUS and DCE-MRI

Figure 4 shows the ROC curves for the different patterns of breast lesions. Table 4 presents the area under the ROC curve (Az), sensitivity, specificity, positive predictive value (PPV), and negative predictive value (NPV). Regardless of breast lesion type, the results of different modalities for differentiating benign and malignant breast lesions showed no significant differences in sensitivity, specificity, PPV, and NPV between CEUS and DCE-MRI (P>0.05 for all). DCE-MRI yielded higher specificity and PPV than CEUS (89.2% vs 81.8%, 85.7% vs 78.4%, respectively), but lower sensitivity and NPV (92.3% vs 94.2%, 94.3% vs 95.3%, respectively), when DCE-MRI and CEUS results for all breast lesions are compared. For mass-like breast lesions, the sensitivity and NPV of CEUS were 92.7% and 95.1%, higher than those of DCE-MRI (82.9% and 94.1%). While for non-mass-like breast lesions, DCE-MRI had obvious advantages in sensitivity, specificity, and PPV.

The results of the analysis for mass-like lesions of different sizes are shown in Table 5. No significant differences in the diagnostic performances of CEUS and DCE-MRI were observed in lesions <10 mm and >20 mm (P= 0.716, P= 0.394). For 10–20 mm breast masses, DCE-MRI had better diagnostic performance in distinguishing benign and malignant lesions than CEUS. Significant differences were found between DCE-MRI and CEUS (P=0.043). Compared with CEUS (0.940, 78.6%, 92.7%, 91.7%, 80.9%, respectively), DCE-MRI showed considerably higher Az, sensitivity, specificity, PPV, and NPV, with values of 0.981, 88.1%, 97.6%, 97.4%, and 88.9%, respectively.

Discussion

In this study, the diagnostic efficacy of CEUS and DCE-MRI was compared in different contrast patterns and

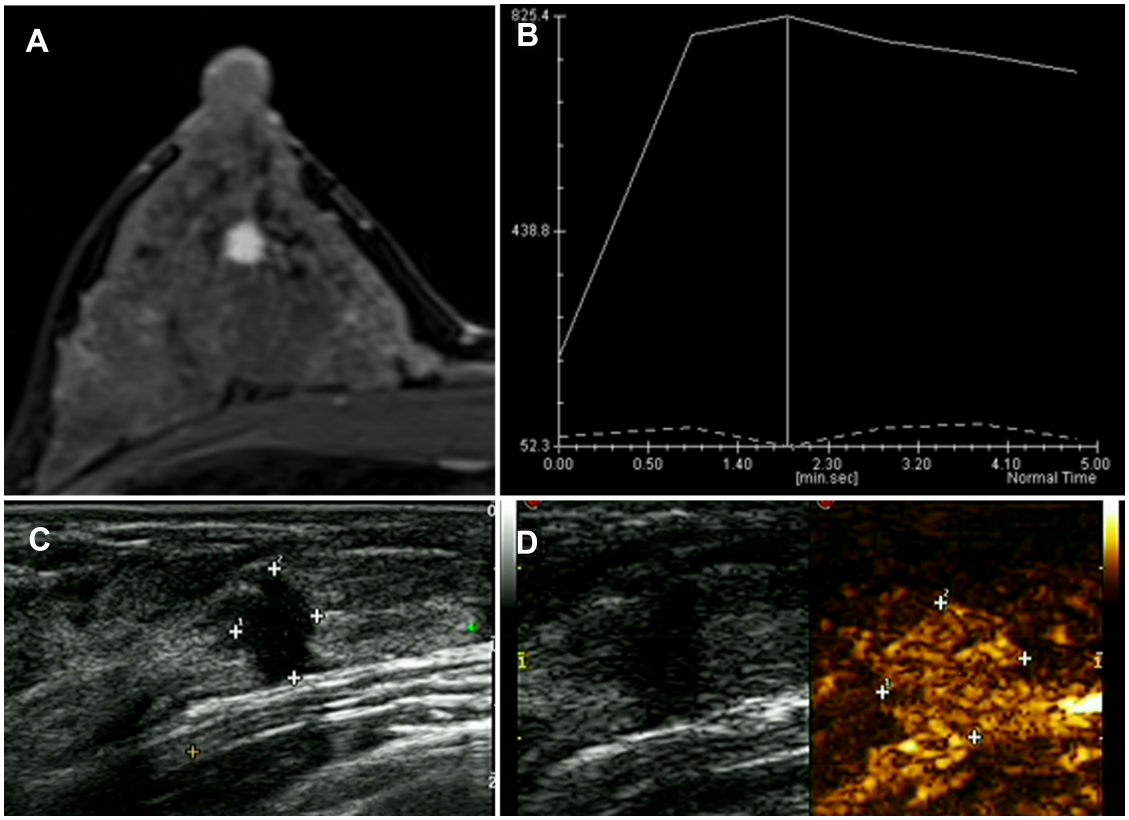

Figure 2 A 35-year-old female patient found a breast lump in the right outer lower quadrant when she made a breast screening. The examination was normal. (**A**) DCE-MRI reported mass-like hyperenhancement. (**B**) The TIC curve showed wash-out type. (**C**) The US presented irregular hypoechoic lesion sized 6*8 mm, and the surrounding tissues were tangled. (**D**) CEUS showed homogeneous enhancement and hyperenhancement. After the enhancement, the border slightly expanded. The pathology result is invasive ductal carcinoma (IDC).

lesions of different sizes. For a distinct contrast pattern, the results showed that CEUS and DCE-MRI maintained good diagnostic accuracy. For mass-like lesions of different sizes (large and small tumors), no significant difference was found between CEUS and DCE-MRI. For a medium-sized mass, although both examination methods exhibited relatively high accuracy, the performance of DCE-MRI was slightly better than that of CEUS.

DCE-MRI showed non-mass-like enhancement of breast lesions, which could be manifested as a mass with visible space on US and CEUS or as a patchy hypoechoic with irregular, unclear borders. Various imaging features can be used for the differential diagnosis of benign and malignant non-mass-like enhancement lesions. Similar to previous studies,[19,20,23] Yang et al.[25] showed that the sensitivity, specificity, and *Az* of DCE-MRI were 90.4%, 47.4%, and 0.802, respectively, for non-mass-like enhancement breast lesions. Zhang et al.[5] analyzed the relevant diagnostic efficacy of CEUS and found that the sensitivity, specificity, and *Az* were 90.0%, 58.1%, and 0.862, respectively, for non-mass-like enhancement breast lesions. In the present study, DCE-MRI has a clear advantage in the diagnosis of non-mass-like enhancement lesions, with an *Az* value of 0.947, which is higher than that of CEUS (0.859). DCE-MRI also had higher sensitivity of 91.7% and specificity of 89.7% than CEUS (75.0% and 76.9%, respectively). However, no statistical difference was found between the two inspection methods. These results are very similar to previous studies.[21–23] CEUS and DCE-MRI have high spatial and temporal resolution and provided a great opportunity for visualization of microcirculation. These two methods facilitate the morphological analysis of cancers as well as the functional evaluation of microcirculation and hemodynamic characteristics. They not only focus on the whole lesion but also the imbalance of tumor microcirculation. Although no statistical difference exists between CEUS and DCE-MRI in differentiating benign and malignant non-mass breast lesions,

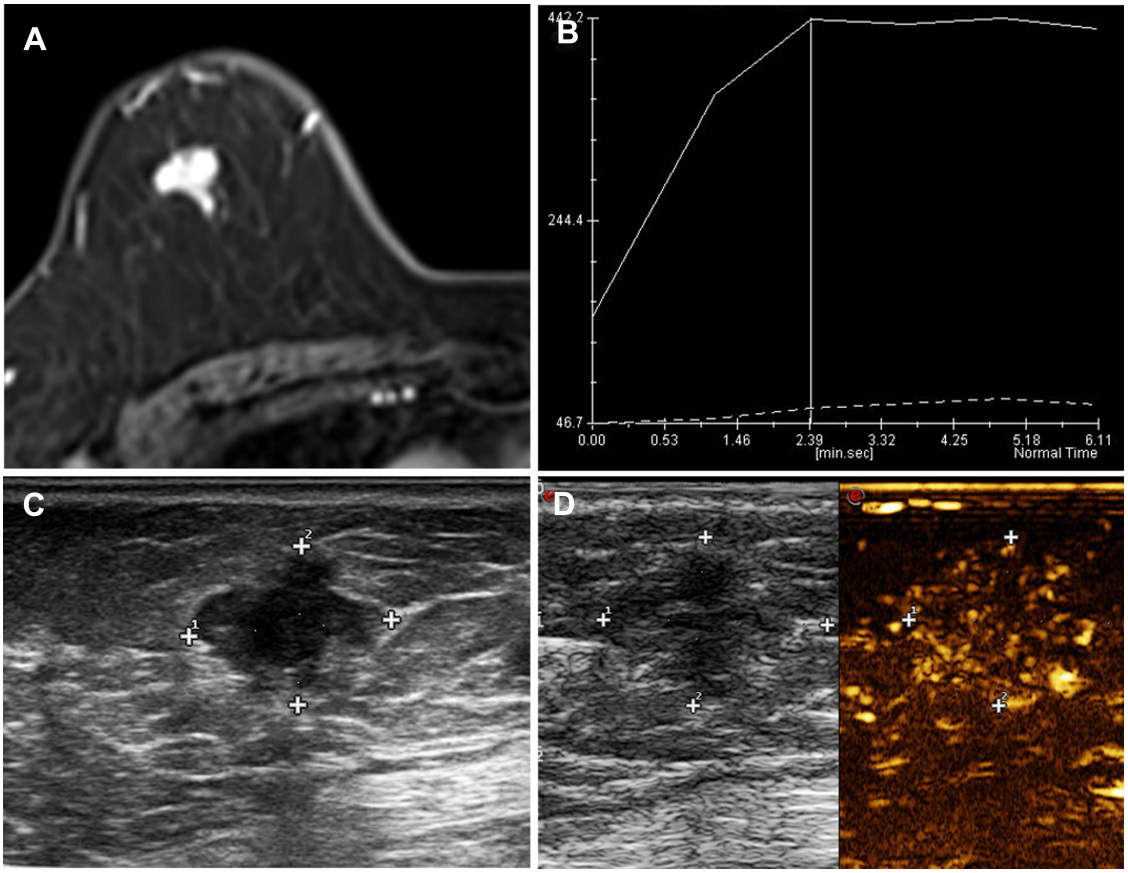

Figure 3 A 66-year-old female patient with a tough nodule in the right upper outer quadrant breast. (**A**) DCE-MRI showed an irregular mass with a size of about 16×11×11 mm and an ADC value of about $0.84\times10^{-3}mm^2/s$. (**B**) After enhancement, the TIC curve was plateau type and the edges were obviously not smooth. (**C**) The US presented an irregular hypoechoic lesion. (**D**) CEUS presented a heterogeneous enhancement and hyperenhancement enhancement; after enhancement, the range enlarged. The pathology result is invasive ductal carcinoma (IDC).

CEUS can be a reliable alternative to MRI for patients with claustrophobia or having internal metal implants.

CEUS and DCE-MRI have higher diagnostic performance in mass-like breast lesions than in non-mass-like enhancement of breast lesions. This finding is consistent with the results of Newburg et al.[4] Conventional US has a poor diagnostic efficiency for the differentiation of benign and malignant breast lesions and has approximately 60% sensitivity and 97% specificity.[12] Angiogenesis is the common characteristic pathological process of most solid tumors,[18,26] and is related to tumor growth, invasion, metastasis, and prognosis.[18,20,27] This phenomenon explains why the application of contrast agents significantly improves the diagnosis of breast lesions. Non-mass-like enhancement breast lesions no longer have the typical two-dimensional graphical features. The hemodynamic characteristics of lesions can be dynamically recorded using the enhanced mode to provide effective diagnostic information.[28] In addition, CEUS can achieve similar effects to DCE-MRI and can be an alternative for patients who are not suitable for DCE-MRI.

The size of mass-like lesions has always been an important part of TNM staging for breast cancer. Pop et al.[29] proposed that MRI more accurately estimates breast tumor size than US or MMG. In the present study, the pathological size was used as the standard for grouping. For small lumps (<10 mm), CEUS showed better sensitivity and specificity than DCE-MRI, but the difference was not significant. For large lumps (>20 mm), both modalities showed good diagnostic performance. This result may be due to the correlation of lesion size with the benign or malignant state. In the diagnosis of medium-sized breast lesions (10–20 mm), DCE-MRI was more advantageous than CEUS, thus contradicting previous studies.[29] This finding can be explained by the characteristics of the pathological progression of benign and malignant

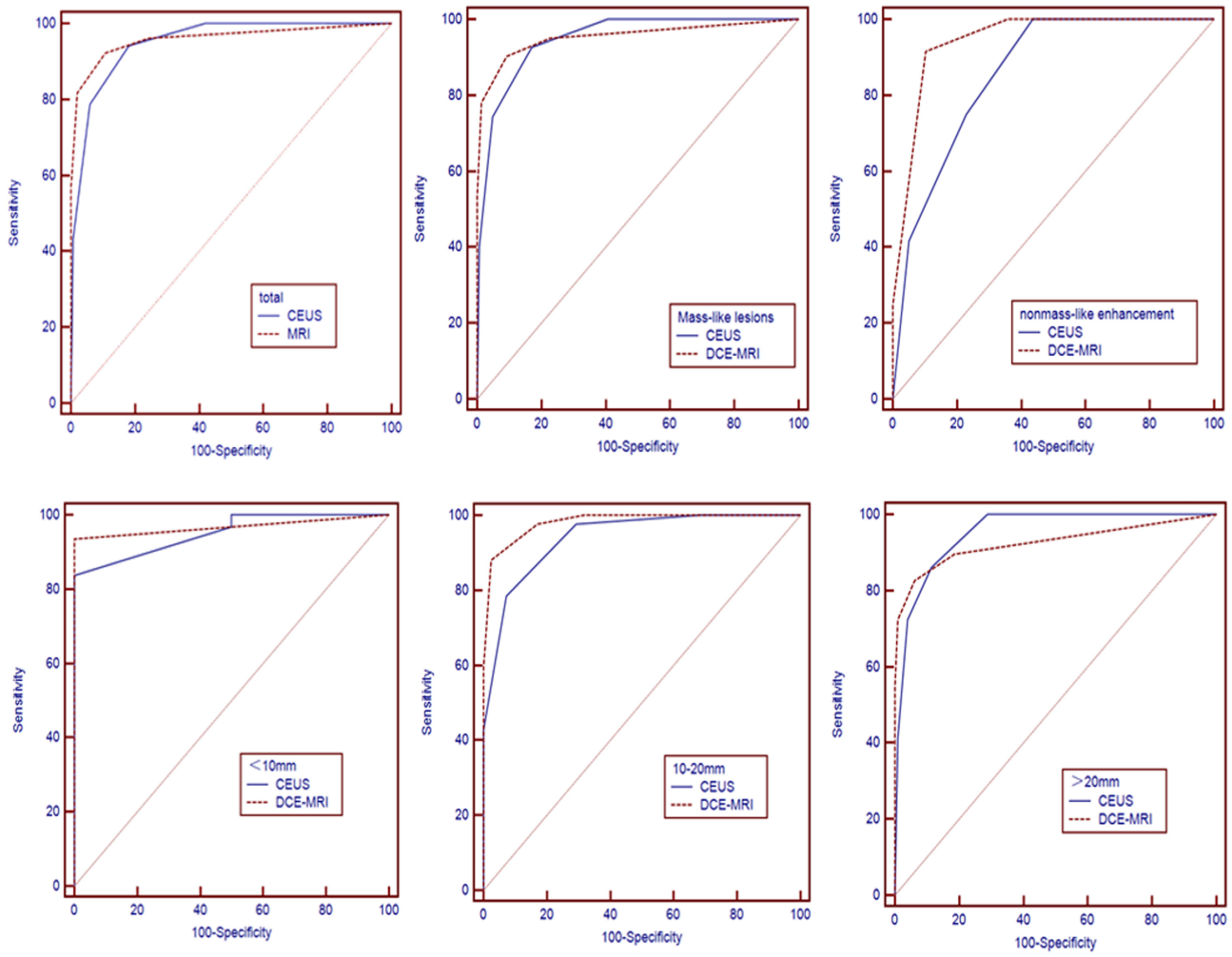

Figure 4 Comparison of diagnostic performance among different modalities for detecting breast lesions in different contrast-enhancement types and mass-like lesions of different sizes.

breast lesions. Benign breast lesions are usually small, grow slowly, and can maintain regular shapes and boundaries during their growth. Malignant lesions usually grow rapidly and are aggressive. Nutrients for early tumor growth are absorbed through molecular exchange.[18–20] When the benign mass grows to a critical size, it may show heterogeneity due to insufficient internal blood supply or may exhibit blood supply characteristics similar to malignant mass nourished by blood vessels. These manifestations on CEUS and DCE-MRI may cause difficulties in the differential diagnosis. CEUS uses a microbubble contrast agent, which only exists in blood vessels. While DCE-MRI uses a micromolecule agent, with an irreplaceable ascendancy that it can enter the intercellular space and present the metabolic characteristics in tumors.[30] This difference probably explains why DCE-MRI can present more image features for the benign and malignant identification of breast lesions at the borderline size and have significant advantages than CEUS.

Our study has several limitations. First, quantitative CEUS was not included in the analysis. Many factors affect the quantitative parameters, such as machine variability, subjective drawing of ROIs, different contrast doses, and type of contrast agents, and patient pharmacokinetics. Therefore, these factors can be applied as comparatively objective parameters in a future study. Second, this study adopted a single-institution, retrospective design. Third, the intra- and inter-observer variabilities were not assessed in the analysis of image features. Fourth, non-mass-like enhancement breast lesions were not classified in detail due to the lack of normalization according to the latest version BI-RADS reporting standardization.[31–33] Fifth,

Table 4 Diagnostic Performance of CEUS and DCE-MRI for Different Enhanced Patterns of Breast Lesions

Group	CEUS					DCE-MRI					*Z*	*P*
	Az (95% CI)	Sensitivity (%)	Specificity (%)	PPV	NPV	*Az* (95% CI)	Sensitivity (%)	Specificity (%)	PPV	NPV		
Total	0.950 (0.916–0.974)	94.2	81.8	78.4	95.3	0.960 (0.928–0.981)	92.3	89.2	85.7	94.3	0.681	0.496
Mass-like lesions	0.947 (0.909–0.973)	92.7	90.2	76.0	95.1	0.954 (0.917–0.977)	82.9	90.7	85.1	94.1	0.400	0.689
Non-mass-like lesions	0.859 (0.733–0.940)	75.0	76.9	41.4	100	0.947 (0.845–0.990)	91.7	89.7	73.3	97.2	1.590	0.119

Abbreviations: *Az*, area under the ROC curve; CI, confidence interval; PPV, positive predictive value; NPV, negative predictive value.

Table 5 Diagnostic Performance of CEUS and DCE-MRI for Different Sizes of Mass-Like Breast Lesions

Group	CEUS					DCE-MRI					*Z*	*P*
	Az (95% CI)	Sensitivity (%)	Specificity (%)	PPV	NPV	*Az* (95% CI)	Sensitivity (%)	Specificity (%)	PPV	NPV		
<10mm	0.952 (0.815–0.996)	96.8	100	96.8	50.0	0.968 (0.839–0.999)	93.5	100	100	50.0	0.363	0.716
10–20mm	0.940 (0.866–0.981)	78.6	92.7	91.7	80.9	0.981 (0.924–0.999)	88.1	97.6	97.4	88.9	2.018	0.043
>20mm	0.951 (0.898–0.982)	86.2	88.7	69.4	95.6	0.926 (0.865–0.965)	82.8	93.8	80.0	94.8	0.852	0.394

Abbreviations: *Az*, area under the ROC curve; CI, confidence interval; PPV, positive predictive value; NPV, negative predictive value.

multifocal and bilateral lesions were not included because only one lesion can be studied at a time on CEUS, whereas the MRI can evaluate both breasts. Therefore, CEUS cannot be completely used to replace MRI in most cases.

In conclusion, for mass-like breast lesions, DCE-MRI showed better diagnostic performance than CEUS in differentiating benign and malignant tumors of medium-sizes (10–20 mm) but not of small (<10 mm) and large (>20 mm) sizes. For non-mass-like lesions, both methods showed similar diagnostic performance. Thus, CEUS is a reliable alternative for those patients who cannot undergo DCE-MRI due to various active or passive reasons. Compared with conventional US, CEUS can effectively improve the efficiency of clinical diagnosis and provide effective auxiliary information for patients with breast diseases to develop personalized diagnosis and treatment plans.

Author Contributions

All authors contributed to data analysis, drafting or revising the article, have agreed on the journal to which the article will be submitted, gave final approval of the version to be published, and agree to be accountable for all aspects of the work. Wei Liu, Min Zong, and Hai-yan Gong contributed equally to this work and should be considered as co-first authors.

Funding

There is no funding to report.

Disclosure

The authors report no conflicts of interest for this work.

References

1. Bray F, Ferlay J, Soerjomataram I, et al. Global cancer statistics 2018: GLOBOCAN estimates of incidence and mortality worldwide for 36 cancers in 185 countries. *CA Cancer J Clin*. 2018;68(6):394–424. doi:10.3322/caac.21492
2. Ginsburg O, Bray F, Coleman MP, et al. The global burden of women's cancers: a grand challenge in global health. *Lancet*. 2017;389(10071):847–860. doi:10.1016/S0140-6736(16)31392-7
3. Avendano D, Marino MA, Leithner D, et al. Limited role of DWI with apparent diffusion coefficient mapping in breast lesions presenting as non-mass enhancement on dynamic contrast-enhanced MRI. *Breast Cancer Res*. 2019;21(1):136. doi:10.1186/s13058-019-1208-y
4. Newburg AR, Chhor CM, Young Lin LL, et al. Magnetic resonance imaging-directed ultrasound imaging of non-mass enhancement in the breast: outcomes and frequency of malignancy. *J Ultrasound Med*. 2017;36(3):493–504. doi:10.7863/ultra.16.03001
5. Zhang W, Xiao X, Xu X, et al. Non-mass breast lesions on ultrasound: feature exploration and multimode ultrasonic diagnosis. *Ultrasound Med Biol*. 2018;44(8):1703–1711. doi:10.1016/j.ultrasmedbio.2018.05.005
6. Lee J, Lee JH, Baik S, et al. Non-mass lesions on screening breast ultrasound. *Med Ultrason*. 2016;18(4):446–451. doi:10.11152/mu-871
7. Aydin H. The MRI characteristics of non-mass enhancement lesions of the breast: associations with malignancy. *Br J Radiol*. 2019;92(1096):20180464. doi:10.1259/bjr.20180464
8. Harbeck N, Gnant M. Breast cancer. *Lancet*. 2017;389(10074):1134–1150. doi:10.1016/S0140-6736(16)31891-8
9. Brem RF, Lenihan MJ, Lieberman J, et al. Screening breast ultrasound: past, present, and future. *AJR Am J Roentgenol*. 2015;204(2):234–240. doi:10.2214/AJR.13.12072
10. Oeffinger KC, Fontham ETH, Etzioni R, et al. Breast cancer screening for women at average risk: 2015 guideline update from the American Cancer Society. *JAMA*. 2015;314(15):1599–1614. doi:10.1001/jama.2015.12783
11. Kuhl CK, Schrading S, Strobel K, et al. Abbreviated breast Magnetic Resonance Imaging (MRI): first postcontrast subtracted images and maximum-intensity projection—a novel approach to breast cancer screening with MRI. *J Clin Oncol*. 2014;32(22):2304–2310. doi:10.1200/JCO.2013.52.5386
12. Guo R, Lu G, Qin B, et al. Ultrasound imaging technologies for breast cancer detection and management: a review. *Ultrasound Med Biol*. 2018;44(1):37–70. doi:10.1016/j.ultrasmedbio.2017.09.012
13. Nelson HD, Fu R, Cantor A, et al. Effectiveness of breast cancer screening: systematic review and meta-analysis to update the 2009 U.S. preventive services task force recommendation. *Ann Intern Med*. 2016;164(4):244–255. doi:10.7326/M15-0969
14. Siu AL; U.S. Preventive Services Task Force. Screening for breast cancer: U.S. preventive services task force recommendation statement. *Ann Intern Med*. 2016;164(4):279–296. doi:10.7326/M15-2886
15. Boughey JC, Ballman KV, Hunt KK, et al. Axillary ultrasound after neoadjuvant chemotherapy and its impact on sentinel lymph node surgery: results from the American College of Surgeons Oncology Group Z1071 trial (alliance). *J Clin Oncol*. 2015;33(30):3386–3393. doi:10.1200/JCO.2014.57.8401
16. Chen S-C, Cheung Y-C, Su C-H, et al. Analysis of sonographic features for the differentiation of benign and malignant breast tumors of different sizes. *Ultrasound Obstet Gynecol*. 2004;23(2):188–193. doi:10.1002/uog.930
17. Lee SH, Chang JM, Kim WH, et al. Added value of shear-wave elastography for evaluation of breast masses detected with screening US imaging. *Radiology*. 2014;273(1):61–69. doi:10.1148/radiol.14132443
18. Camare C, Pucelle M, Negre-Salvayre A, et al. Angiogenesis in the atherosclerotic plaque. *Redox Biol*. 2017;12:18–34. doi:10.1016/j.redox.2017.01.007
19. Guo L, Harari E, Virmani R, et al. Linking hemorrhage, angiogenesis, macrophages, and iron metabolism in atherosclerotic vascular diseases. *Arterioscler Thromb Vasc Biol*. 2017;37(4):e33–e39. doi:10.1161/ATVBAHA.117.309045
20. Maeda H, Wu J, Sawa T, et al. Tumor vascular permeability and the EPR effect in macromolecular therapeutics: a review. *J Control Release*. 2000;65(1–2):271–284. doi:10.1016/S0168-3659(99)00248-5
21. Ricci P, Cantisani V, Ballesio L, et al. Benign and malignant breast lesions: efficacy of real time contrast-enhanced ultrasound vs. magnetic resonance imaging. *Ultraschall Med*. 2007;28(1):57–62. doi:10.1055/s-2006-927226
22. Du J, Wang L, Wan C-F, et al. Differentiating benign from malignant solid breast lesions: combined utility of conventional ultrasound and contrast-enhanced ultrasound in comparison with magnetic resonance imaging. *Eur J Radiol*. 2012;81(12):3890–3899. doi:10.1016/j.ejrad.2012.09.004
23. Li C, Yao M, Shao S, et al. Diagnostic efficacy of contrast-enhanced ultrasound for breast lesions of different sizes: a comparative study with magnetic resonance imaging. *Br J Radiol*. 2020;93(1110):20190932. doi:10.1259/bjr.20190932

24. Xiang W, Huang Z, Tang C, et al. Use of ultrasound combined with magnetic resonance imaging for diagnosis of breast masses and fibroids. *J Int Med Res*. 2019;47(7):3070–3078. doi:10.1177/0300060519848611
25. Yang X, Dong M, Li S, et al. Diffusion-weighted imaging or dynamic contrast-enhanced curve: a retrospective analysis of contrast-enhanced magnetic resonance imaging–based differential diagnoses of benign and malignant breast lesions. *Eur Radiol*. 2020;30(9):4795–4805. doi:10.1007/s00330-020-06883-w
26. Aalders KC, Tryfonidis K, Senkus E, et al. Anti-angiogenic treatment in breast cancer: facts, successes, failures and future perspectives. *Cancer Treat Rev*. 2017;53:98–110. doi:10.1016/j.ctrv.2016.12.009
27. Schneider BP, Miller KD. Angiogenesis of breast cancer. *J Clin Oncol*. 2005;23(8):1782–1790. doi:10.1200/JCO.2005.12.017
28. Nykanen A, Arponen O, Sutela A, et al. Is there a role for contrast-enhanced ultrasound in the detection and biopsy of MRI only visible breast lesions? *Radiol Oncol*. 2017;51(4):386–392. doi:10.1515/raon-2017-0049
29. Pop C-F, Stanciu-Pop C, Drisis S, et al. The impact of breast MRI workup on tumor size assessment and surgical planning in patients with early breast cancer. *Breast J*. 2018;24(6):927–933. doi:10.1111/tbj.13104
30. Kuhl CK. Abbreviated Magnetic Resonance Imaging (MRI) for breast cancer screening: rationale, concept, and transfer to clinical practice. *Annu Rev Med*. 2019;70(1):501–519. doi:10.1146/annurev-med-121417-100403
31. Lunkiewicz M, Forte S, Freiwald B, et al. Interobserver variability and likelihood of malignancy for fifth edition BI-RADS MRI descriptors in non-mass breast lesions. *Eur Radiol*. 2020;30(1):77–86. doi:10.1007/s00330-019-06312-7
32. Krammer J, Zolotarev S, Hillman I, et al. Evaluation of a new image reconstruction method for digital breast tomosynthesis: effects on the visibility of breast lesions and breast density. *Br J Radiol*. 2019;92(1103):20190345. doi:10.1259/bjr.20190345
33. Lee JM, Ichikawa L, Valencia E, et al. Performance benchmarks for screening breast MR imaging in community practice. *Radiology*. 2017;285(1):44–52. doi:10.1148/radiol.2017162033